AGU ADVANCING EARTH AND SPACE SCIENCE

Geophysical Research Letters

RESEARCH LETTER
10.1029/2021GL094446

Key Points:

- The thermal stability of FeOOH has been investigated by shock recovery experiments up to ~70 GPa and ~2,750 K
- FeOOH partially decomposes and releases water and oxygen in the mid-lower mantle
- The deoxygenation of FeOOH is a potential sporadic oxygen source for the Great Oxidation Event of Earth

Supporting Information:

Supporting Information may be found in the online version of this article.

Correspondence to:

Y. Zhang,
zhangyoujun@scu.edu.cn

Citation:

Gan, B., Zhang, Y., Huang, Y., Li, X., Wang, Q., Li, J., et al. (2021). Partial deoxygenation and dehydration of ferric oxyhydroxide in Earth's subducting slabs. *Geophysical Research Letters*, *48*, e2021GL094446. https://doi.org/10.1029/2021GL094446

Received 25 MAY 2021
Accepted 14 AUG 2021

Partial Deoxygenation and Dehydration of Ferric Oxyhydroxide in Earth's Subducting Slabs

Bo Gan[1,2], Youjun Zhang[1,3], Yuqian Huang[1], Xiaohong Li[1], Qiming Wang[1], Jun Li[4], Yukuai Zhuang[1], Yun Liu[3,5], and Gang Jiang[1]

[1]Institute of Atomic and Molecular Physics, Sichuan University, Chengdu, China, [2]Key Laboratory of Deep Earth Science and Engineering, Ministry of Education, Sichuan University, Chengdu, China, [3]International Center for Planetary Science, College of Earth Sciences, Chengdu University of Technology, Chengdu, China, [4]National Key Laboratory for Shock Wave and Detonation Physics, Institute of Fluid Physics, Mianyang, China, [5]Institute of Geochemistry, Chinese Academy of Sciences, Guiyang, China

Abstract The thermal stability of hydrous minerals in Earth's deep interior is key to understanding the evolution and physicochemical states of the planet. The recently discovered pyrite-type (Py) FeO_2H_x ($x \leq 1$) phase, which can be transformed from α/ε-FeOOH at ~80 GPa, is believed to be a crucial candidate in transporting water and hydrogen to the lowermost mantle through subducting slabs. Here, we examined the stability and decomposition behavior of FeOOH through a set of shock-recovery experiments up to ~70 GPa and ~2,750 K. Our results show that FeOOH partially decomposes to iron oxides Fe_2O_3 and Fe_3O_4 at 35–70 GPa and 1,150–2,750 K, which indicates that H_2O and O_2 are released during the decomposition of FeOOH in subducting slabs. The released H_2O and O_2 may have altered the physical and chemical properties of the surrounding mantle and contributed to the oxidation of surface Earth.

Plain Language Summary The mineral goethite (α-FeOOH), a primary component of rusts and bog iron ores, is widespread on our planet. Early studies show that FeOOH polymorphs could transport water and hydrogen to the lowermost mantle when the minerals are transformed into hydrogen-bearing iron peroxides at ~1,800 km depths. However, the thermal stability of FeOOH at the mid-lower mantle equivalent pressure-temperature conditions is poorly known. Here, we used a shock-recovery approach to examine the stability of FeOOH at pressures up to ~70 GPa and temperatures to ~2,750 K. Our results show that FeOOH partially decomposes to form hematite and magnetite, releasing water and oxygen at the equivalent pressure-temperature conditions of a subducting slab in the mid-lower mantle, thus indicating a narrower FeOOH-stable region in the lower mantle than previously proposed. The released oxygen via FeOOH decomposition may have provided extra oxidation power for the long-term oxidation of Earth's surface.

1. Introduction

Hydrous minerals or their water-bearing phases are widely recognized as potential water, oxygen, and hydrogen carriers in Earth's interior (Nishi, 2015; Ohtani, 2020; A. B. Thompson, 1992). They can dehydrate and/or deoxygenate under high pressure-temperature (*P-T*) conditions, thereby affecting the key physical and chemical properties of mantle minerals (e.g., Chang et al., 2017; Hou et al., 2021; Hwang et al., 2017; Jacobsen & Smyth, 2006; Jacobsen et al., 2004; J. Liu et al., 2020; Mao et al., 2017; Schmandt et al., 2014). Extensive studies have been conducted to examine the stability fields of various hydrous phases, such as dense hydrous magnesium silicates (DHMSs) (e.g., Komabayashi et al., 2005; Nishi et al., 2014; Ohira et al., 2014; Pamato et al., 2015; Y. Zhang et al., 2014), hydrous bridgmanite (Fu et al., 2019), phase δ-AlOOH (Ohtani et al., 2001), and iron oxyhydroxide (Yoshino et al., 2019) minerals. Some aluminum-rich DHMSs can remain stable along the mantle geotherm in the lower mantle (e.g., Ohira et al., 2014; Pamato et al., 2015), suggesting that water might be stored in the deep interior (e.g., Kohlstedt et al., 1996; Nishi, 2015; Ono, 1998; Pearson et al., 2014; Smyth, 1987).

Due to similar crystallographic frameworks with strong hydrogen bonds, the solid-solution mixtures of isostructural ε-FeOOH, δ-AlOOH, and $MgSiO_4H_2$ are proposed to be water carriers to the lower mantle

(Nishi et al., 2014, 2019; E. C. Thompson et al., 2020; Xu et al., 2019). FeOOH is one of the important hydrous phases in the subducting slabs of the Earth's mantle (e.g., Hu et al., 2016; Nishi et al., 2017), containing nominally 10.13 wt.% water. Natural FeOOH includes goethite (α-FeOOH), akaganeite (β-FeOOH), and lepidocrocite (γ-FeOOH), which can be transferred to the high-pressure polymorphs of ε-FeOOH with a $CaCl_2$-type structure (space group $P2_1nm$) at ~7 GPa (Suzuki, 2010). The stability, structural, physical, and chemical properties of ε-FeOOH at high *P-T* conditions have attracted intensive interest (e.g., Ikeda et al., 2019; Nishihara & Matsukage, 2016; E. C. Thompson et al., 2020).

Yoshino et al. (2019) studied the dehydration behavior of ε-FeOOH up to ~20 GPa and found that its dehydration temperature increased with increasing pressure. Hu et al. (2016, 2017) and Nishi et al. (2017) investigated the stability of ε-FeOOH using laser-heated diamond anvil cells (LH-DACs) under the relevant *P-T* conditions of the lowermost mantle and reported that ε-FeOOH could remain stable until it descended to a depth of ~1,800 km and then transformed into stable Py-FeO_2H_x ($x \leq 1$, space group $Pa\bar{3}$). The results of first-principles calculations at 0 K also supported that ε-FeOOH remains stable before transforming to Py-FeO_2H_x (e.g., Lu & Chen, 2018; Nishi et al., 2017). The fully dehydrogenated Py-FeO_2H_x would possibly decompose in the uprising plumes, which may provide a sporadic oxygen source for the Great Oxidation Event (GOE; Hu et al., 2016). Where, the GOE is the first long-term oxygenation event of Earth's atmosphere at ~2.3–2.5 billion years (Gyr) ago based on the evidence of Earth surface oxygenation (e.g., Canfield, 2004; Farquhar et al., 2000; Guo et al., 2009; Holland, 2002). Furthermore, recent LH-DAC experiments indicated that ε-FeOOH may partially dehydrate to form a new hydrous iron oxide η-$Fe_{12}O_{19}H_2$ (H. Chen et al., 2020) or decompose to various iron oxides (Fe_2O_3, Fe_5O_7, Fe_7O_{10}, and $Fe_{6.32}O_9$) and an oxygen-rich fluid in the slabs present at the mid-lower mantle (Koemets et al., 2021), suggesting that FeOOH may become unstable and the oxygen-rich fluid may contribute to the GOE. These results indicate that a sturdy approach is urgently needed to further investigate the thermal stability of FeOOH at the relevant *P-T* conditions of the mid-lower mantle and to explore how oxygen and water are released from the Fe-O-H system.

Here, we investigated the stability and decomposition reaction of FeOOH under high *P-T* conditions by shock recovery experiments. Natural goethite (α-FeOOH), as one of the most widespread forms of iron (III) oxyhydroxide in ore deposits, sediments, and terrestrial soils, was shocked up to ~70 GPa and ~2,750 K using a two-stage light-gas gun. The present experimental results suggest that FeOOH at conditions relevant to the subducting slabs is unstable and may decompose and release water and oxygen in the mid-lower mantle. A portion of FeOOH in the very cold subducting slabs may remain stable down to the deep-lower mantle. These results provide key information that is essential to understanding the evolution of Earth's atmosphere and geological processes in Earth's interior.

2. Materials and Methods

Natural goethite was used as the starting material, and its chemical composition was analyzed using X-ray diffraction (XRD) and an electron probe microanalyzer (EPMA, type: SHIMADZU, EPMA-1720H). Its XRD pattern matches the α phase (*Pbnm*) with a unit cell volume of 138.6 $Å^3$ under ambient conditions (Figure S1a). The EPMA results indicate that the sample is homogeneous and mainly contains ~95 wt.% FeOOH and ~3 wt.% SiO_2 impurities (Figure S1b and Table S1). The density of each sample was measured by the Archimedean method and ranged between 3.902 and 3.932 g/cm^3, falling ~8% lower than the ideal density of 4.26 g/cm^3 for the pure α-FeOOH phase due to impurities and possible porosity in natural samples (Wiethoff et al., 2017).

Shock experiments were carried out using a 25-mm two-stage light-gas gun at the Institute of Atomic and Molecular Physics, Sichuan University. A schematic diagram of the shock recovery experiment is shown in Figure S2. Aluminum (Al) and copper (Cu) were used as the flyer plate with a diameter of ~24 mm and a thickness of ~4 mm. The impact velocity of the flyer was measured by an electromagnetic method within an ~0.5% uncertainty. The sample (~12 mm diameter, ~2 mm thick) was sealed in a Cu container, and the sample chamber was located ~3 mm away from the impact surface. The shock pressure was calculated using the impedance matching method based on the measured impact velocity and the known Hugoniot relations of the flyer and container (Table S2) (Marsh, 1980; Seiler & Igra, 2016). The shock temperature was estimated using a thermodynamic equation based on the equation of the state of FeOOH

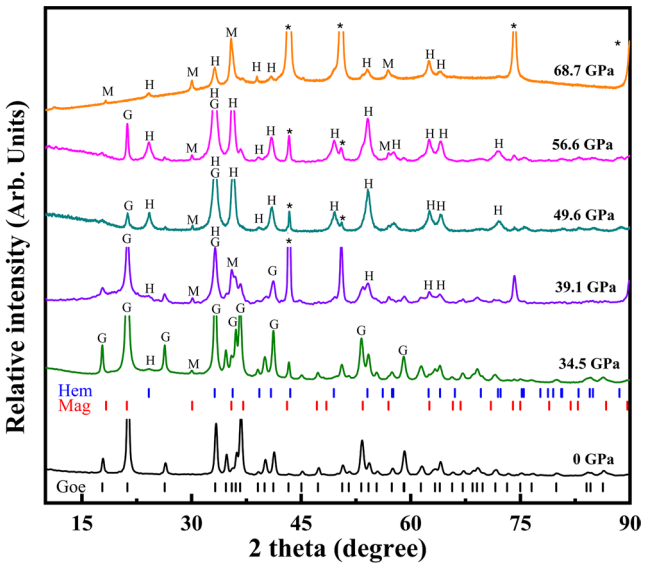

Figure 1. X-ray diffraction patterns of the used goethite under ambient conditions and the postshock samples. Symbols of G, H, M, and * represent the diffraction indices assigned for goethite, hematite, magnetite, and Cu, respectively. Cu may be involved from the container in the process of shock recovery experiments or cutting by a lathe (Sekine et al., 2015). Goe, goethite; Hem, hematite; and Mag, magnetite.

(see Supporting Information S1) (Brown & McQueen, 1986; Gleason et al., 2008; Majzlan et al., 2003; McQueen et al., 1970). A typical impedance matching diagram shows the pressure and temperature histories in the sample under multiple reverberation shock waves (Figure S3).

Five shock recovery experiments were performed in which the impact velocity ranged from ~2.04 to 2.67 km/s. The experimental conditions, shock pressures, and estimated shock temperatures ($T_{est.}$) are listed in Table S2. Our $T_{est.}$ in shocked FeOOH is comparable to that of iron-bearing minerals under shock loading (see Supporting Information S1) (X. Chen et al., 2006; Martinez et al., 1995; F. Zhang & Sekine, 2007). After shots, the recovered containers were cut open using a lathe. We successfully recovered postshock samples at shock pressures of 34.5–68.7 GPa. The recovered samples were investigated using XRD, scanning electron microscopy (SEM) coupled with energy dispersive spectrometry (EDS), and thermal analysis, including thermal gravimetry (TG), derivative thermogravimetric analysis (DTG), and differential scanning calorimetry (DSC).

3. Results

3.1. Decomposition of FeOOH Under Shock Loading

Goethite was shocked to 34.5–68.7 GPa in the present study, where the pressures were substantially higher than the phase boundary between α and ε-FeOOH (e.g., Dyuzheva et al., 2006; K. Liu et al., 2019). After recovery from shock compression, some of the postshock samples were ground into powders, and their phases were identified using XRD with an X-ray wavelength of 1.54 Å (Figure 1). We observed trace amounts of hematite and magnetite for the sample recovered from ~34.5 GPa, indicated by the diffraction peaks at 2θ of 24.15 and 30.08°, respectively, suggesting that ε-FeOOH began to decompose into Fe_3O_4 and Fe_2O_3. With increasing shock pressure, the diffraction peaks of magnetite and hematite were clearly observed. The sample recovered from ~68.7 GPa had almost entirely decomposed, and the goethite component disappeared. The identified phases are listed in Table S2.

The XRD patterns unambiguously indicate that ε-FeOOH decomposes into Fe_3O_4 and Fe_2O_3 at pressures of 35–70 GPa and temperatures of 1,150–2,750 K. Considering the chemical valence equilibrium in FeOOH, the chemical reactions can be described below:

$$2FeOOH \rightarrow Fe_2O_3 + H_2O \quad (1)$$

$$12FeOOH \rightarrow 4Fe_3O_4 + 6H_2O + O_2 \quad (2)$$

$$6Fe_2O_3 \rightarrow 4Fe_3O_4 + O_2 \quad (3)$$

where Fe_2O_3 could be directly formed by the dehydration of FeOOH (Reaction 1) (e.g., Yoshino et al., 2019; W.-J. Zhang et al., 2010). Meanwhile, recent in situ XRD studies showed that FeOOH may partially dehydrate to form the η-$Fe_{12}O_{19}H_2$ at 60–70 GPa and 1,400–1,950 K (H. Chen et al., 2020). The η-$Fe_{12}O_{19}H_2$ can be written as a form of $6Fe_2O_3{\cdot}H_2O$, suggesting that the dehydration process of FeOOH may also occur through an intermediate phase $Fe_{12}O_{19}H_2$ to indirectly form Fe_2O_3 and H_2O (12FeOOH → $Fe_{12}O_{19}H_2$ + $5H_2O$→$6Fe_2O_3$ + $6H_2O$) (Gualtieri & Venturelli, 1999; Wolska, 1988; Wolska & Schwertmann, 1989). In this case, the η-$Fe_{12}O_{19}H_2$ might be formed during shock loading. However, it could not be quenchable to ambient conditions based on our chemical analyses of the postshock samples.

FeOOH was also decomposed with the formation of Fe_3O_4, H_2O, and O_2 in shock recovery experiments (Reaction 2), where partial Fe^{3+} converted to Fe^{2+} during the long-range nature of cation and proton migration in the dehydration process of FeOOH (Ibrahim et al., 1994; Özdemir & Dunlop, 2000). On the other

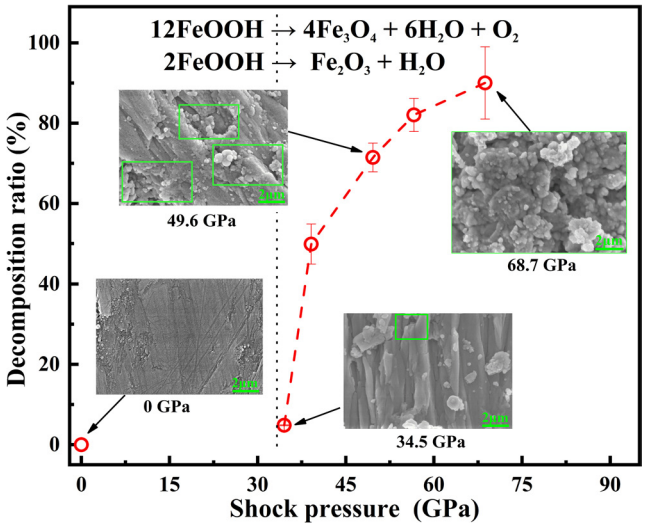

Figure 2. Decomposition ratio of FeOOH as a function of shock pressure. Scanning electron microscopy images show the starting goethite and selected postshock samples (e.g., ~34.5, 49.6, and 68.7 GPa). Some voids were formed by the decomposition of FeOOH, as shown in the open green rectangles.

hand, a self-redox reaction in Fe_2O_3 has been observed at pressures above 60 GPa and temperatures of 2,000 K, forming an unusual Fe_5O_7 phase with the release of oxygen ($10Fe_2O_3 \rightarrow 4Fe_5O_7 + O_2$) (Bykova et al., 2016). Watanabe and Ishii (1995) proposed a mechanism for the transformation from Fe_2O_3 to Fe_3O_4, which occurs by the restacking sequence of oxygen layers, removal of oxygen, and migration of iron ions. These studies indicate that Fe_3O_4 may also be produced from the decomposition of Fe_2O_3 with the direct involvement or facilitation of H_2O after the dehydration of FeOOH. Therefore, Fe_3O_4 may be formed from both the direct decomposition of FeOOH (Reaction 2) and/or a self-redox of Fe_2O_3 (Reaction 3).

3.2. Thermal Analyses and SEM Observations With EDS

We analyzed the pyrolysis characteristics of the starting goethite and the postshock samples using TG, DTG, and DSC (Figure S4). The TG curves exhibit a sharp decrease in weight at 460–620 K due to the dehydration of goethite (e.g., Gualtieri & Venturelli, 1999; Morris & Lauer, 1981; Walter et al., 2001). We calculated the amount of residual goethite in the postshock samples according to their weight losses upon heating and then calculated the decomposition ratio of FeOOH at high *P-T* conditions (Figure 2 and Table S2). The results show that the decomposition ratio increases rapidly with increasing shock pressures from ~35 to ~45 GPa and then, slowly with increasing shock pressures above ~45 GPa (Figure 2). Our results unambiguously indicate that the decomposition of FeOOH starts at ~35 GPa and is completed above 90% at ~70 GPa.

The morphologies of the starting goethite and postshock samples were investigated by SEM coupled with EDS. There were no obvious voids or small particles in the starting goethite (Figure 2). After recovery from a shock pressure of ~34.5 GPa, voids could be observed in the postshock sample, and their size and proportion increase dramatically with increasing shock pressures (Figure 2). These results imply that the decomposition reaction of FeOOH under high *P-T* conditions begins locally and that part of the solid products will form small particles associated with the loss of H_2O and O_2. This is well supported by the EDS results (Figure S5), which show that the mass ratio of iron to oxygen in the postshock samples increases from 1.66 to 2.48 with increasing pressure from 34.5 to 56.6 GPa.

3.3. High *P-T* Phase Diagram of FeOOH

The *P-T* phase diagram of FeOOH can be established by combining the present shock recovery experiments and previous studies (Figure 3). α-FeOOH is the most thermodynamically stable form of iron oxyhydroxide under ambient conditions. At ~7 GPa, α-FeOOH undergoes a first-order phase transition to form high-pressure ε-FeOOH (e.g., Voigt & Will, 1981; Wiethoff et al., 2017). α- and ε-FeOOH undergo dehydration reactions to form hematite and water at high temperatures within the pressure range of ~20 GPa, and the dehydration temperatures increase with increasing pressure (Gleason et al., 2008; Yoshino et al., 2019). Under the high *P-T* conditions of 35–70 GPa and 1,150–2,750 K, our results show that ε-FeOOH partially decomposes into Fe oxides (Fe_2O_3, Fe_3O_4), H_2O, and O_2. Our observations are overall consistent with recent observations in LH-DACs experiments by Koemets et al. (2021); they observed that ε-FeOOH decomposed into various iron oxides (e.g., Fe_2O_3, Fe_3O_4, Fe_5O_7, Fe_7O_{10}, and $Fe_{6.32}O_9$) and an oxygen-rich fluid in the pressure range of 40–80 GPa and at temperatures of 1,200–2,100 K. At higher pressures up to ~80 GPa, the surviving ε-FeOOH may transform into Py-FeO_2H_x ($x \leq 1$) (e.g., Hu et al., 2016; Nishi et al., 2017), which remains stable at high *P-T* conditions up to 1,500 K at 129 GPa and 2,400 K at 111 GPa (Nishi et al., 2017).

The thermal stability of FeOOH in Earth's mantle can be evaluated by comparing its *P-T* phase diagram with some modeled geotherms and subducting slab temperatures (Katsura et al., 2010; Komabayashi et al., 2004; Maeda et al., 2017) (Figure 3). Our study indicates that FeOOH is unstable in cold and hot subducting slabs at a depth of ~900 km and partially decomposes to form H_2O and O_2. However, at relatively low

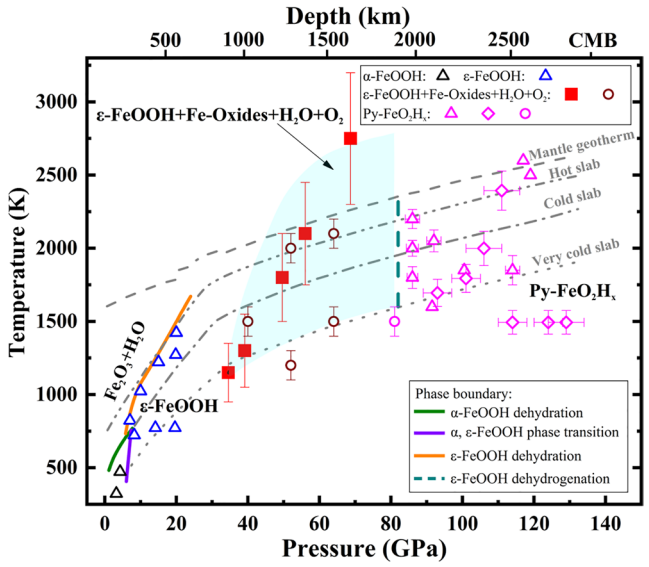

Figure 3. *P-T* phase diagram of FeOOH and its thermal stability under relevant conditions of the subducting slabs. Open black triangles are α-FeOOH (Wiethoff et al., 2017); open blue triangles are ε-FeOOH (Yoshino et al., 2019); solid red squares (this study), and open wine circles (Koemets et al., 2021) indicate that ε-FeOOH partially decomposes into Fe oxides, H_2O, and O_2. Open carmine triangles (Hu et al., 2016, 2017), diamonds (Nishi et al., 2017), and circles (Koemets et al., 2021) represent Py-FeO_2H_x ($x \leq 1$); solid green and violet lines represent the dehydration boundary of α-FeOOH and the phase boundary between α-FeOOH and ε-FeOOH, respectively (Voigt & Will, 1981). The solid orange line is the dehydration boundary of ε-FeOOH (Yoshino et al., 2019). The dashed cyan line is the dehydrogenation boundary of ε-FeOOH (Hu et al., 2016). The dashed gray line represents the proposed mantle geotherm (Katsura et al., 2010); and the double dots, dotted dashed, and dotted lines represent slab geotherms based on hypothetical models of hot, cold, and very cold slabs, respectively (Komabayashi et al., 2004; Maeda et al., 2017).

temperatures and high pressures, the decomposition ratio remains very low (e.g., ~5% at conditions of 1,150 K at 35 GPa), implying that FeOOH may survive under the *P-T* conditions of very cold subducting slabs.

4. Discussion

The preserved earliest marine sediments indicate that Earth's biosphere is driven by anaerobic metabolisms before oxygen is available in the Fe(II)-rich Precambrian environment (Canfield et al., 2006), and one of the most active ecosystems is Fe^{2+} oxidation by anoxygenic photosynthesis (Heising et al., 1999; Jiao et al., 2005; Straub et al., 1999; Widdel et al., 1993). Fe^{2+}-oxidizing microorganisms utilized light energy to oxidize Fe^{2+} and fixed CO_2 into biomass, resulting in the formation of FeOOH (Figure 4) (Canfield et al., 2006; Croal et al., 2004; Kappler & Newman, 2004; Weber et al., 2006), as shown below.

$$HCO_3^- + 4Fe^{2+} + 6H_2O \rightarrow CH_2O + 4FeOOH + 7H^+ \quad (4)$$

where CH_2O denotes the produced biomass in this microbial metabolic process. The GOE as a protracted process (Konhauser et al., 2011), is generally considered to be related to the burial of biomass because cyanobacteria can produce oxygen by photosynthesis ($CO_2 + H_2O \rightarrow CH_2O + O_2$) (Eguchi et al., 2020; Karhu & Holland, 1996; Lyons et al., 2014). In addition to this direct origin of the oxygen from the marine photic zone, the decomposition of the subducted FeOOH may provide an extra source of oxygen.

A transition from stagnant/sluggish lid to plate tectonics and the rapid emergence of subaerial continents and major glaciations have been proposed for around 2.5 Gyr ago (Bindeman et al., 2018; Condie et al., 2016; Gumsley et al., 2017). These events would have enhanced plate tectonic activity. Thus, a large amount of the accumulated FeOOH would descend to the Earth's interior through slab subduction. It would take less than 0.1 Gyr for the subducted FeOOH to reach a depth of 900 km if we assume a sinking speed of ~1.2 cm/year (van der Meer et al., 2010). Our results show that the subducted FeOOH could release H_2O and O_2 at the depth of ~900 km (Figure 4). Besides, if FeOOH was occasionally swept up by upwelling mantle plumes or other large-scale mantle dynamic processes, it would decompose and release H_2O and O_2. These H_2O and O_2 may lead to rapid oxidization of the mantle and strongly reduce the reducing gases emanating from the solid Earth (e.g., CH_4, CO, and H_2). Thus, the consumption of photosynthetic oxygen was decreased and a net increase of atmospheric oxygen could trigger the GOE. Furthermore, recent studies indicated that the GOE is coincident with the formation of numerous large igneous provinces (Ernst & Bleeker, 2010; Gumsley et al., 2017) and massive mantle degassing occurred around 2.5 Gyr ago (Avice et al., 2017, 2018). Therefore, a considerable part of the O_2 released from FeOOH may return to the Earth's surface through mantle degassing and volcano eruption, which directly contributes to the increase in atmospheric oxygen concentration.

H_2O released from FeOOH may also be incorporated into some mafic crustal rocks (Figure 4) (Nishi, 2015), indicating that FeOOH has an important role in subducting slabs to transport water into the mid-lower mantle. In addition, the decomposition temperature of FeOOH is slightly lower than that of some very cold subducting slabs (Figure 3). Recent high *P-T* experiments showed that FeOOH could form solid solutions with the $CaCl_2$-type phases (e.g., δ-AlOOH and $MgSiO_4H_2$) and/or α-PbO_2 structure phases (e.g., SiO_2 and TiO_2) over a wide composition range and then remain stable at higher temperatures (e.g., X. Liu et al., 2018; Nishi et al., 2019; Nishihara & Matsukage, 2016; Ohira et al., 2014; Panero & Caracas, 2017; Xu et al., 2019; Yuan et al., 2019). Therefore, as FeOOH is present in hydrous sediments, peridotite, and mid-ocean ridge basalt compositions, it may be thermodynamically stable in some very cold subducting slabs and likely transport water into the deep lower mantle.

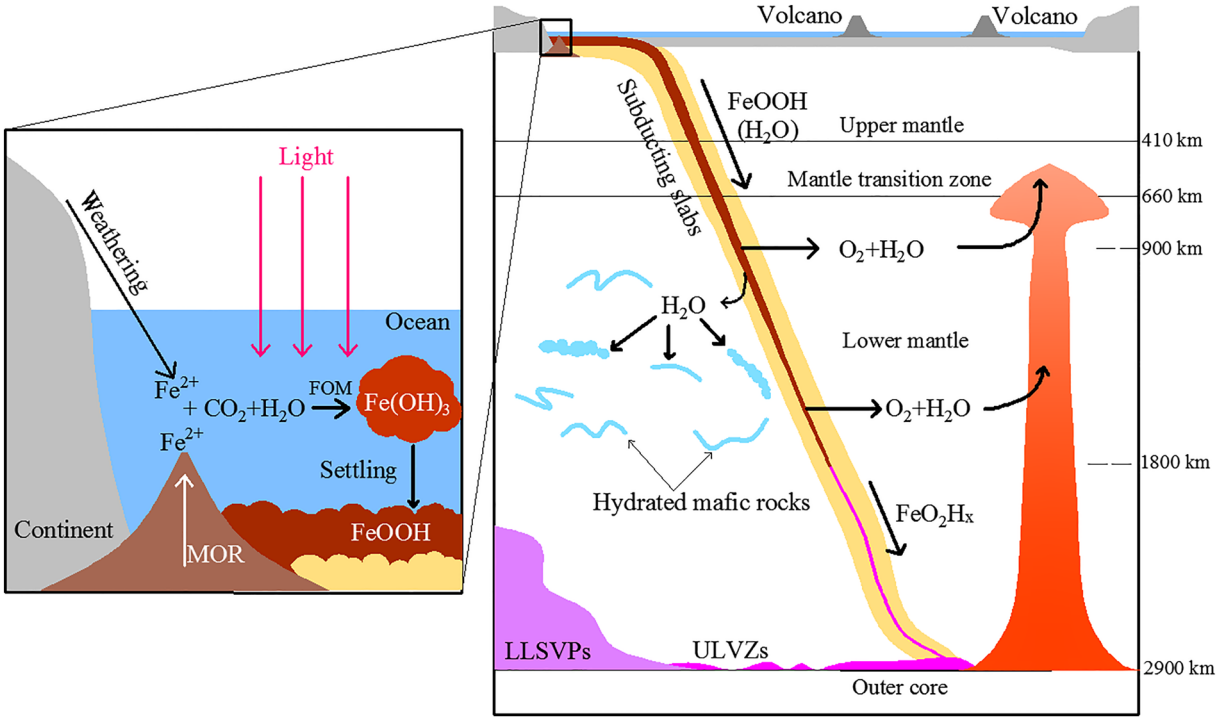

Figure 4. Schematic diagram of the formation and evolution of FeOOH. Left inset: FeOOH was formed in an early Fe^{2+}-rich and oxygen-free environment; in the photic zone of the oceans at 3.8 Gyr ago, Fe^{2+}-oxidizing microorganisms (FOM) utilized light energy to oxidize Fe^{2+} (from the weathering of continental rocks and the mid-ocean ridge [MOR] hydrothermal circulation) and fixed CO_2 into biomass, resulting in the formation of poorly crystalline Fe^{3+} oxides ($Fe(OH)_3$) (Canfield et al., 2006; Weber et al., 2006); $Fe(OH)_3$ subsequently transformed into FeOOH (crimson) in the presence of metabolically active FOM and settled into the deep ocean (Croal et al., 2004; Kappler & Newman, 2004). Right inset: the influence of FeOOH's evolution on geophysical and geochemical processes in Earth; FeOOH (crimson belt) could be carried into the mantle with subducting slabs (yellow area) by plate tectonics; at a depth of ~900 km, FeOOH in the subducting slabs started to release H_2O and O_2, which may occur by upwelling mantle plumes (light red) and plate tectonics (mantle degassing, eruptions of the volcano, etc.) back to Earth's surface. In addition, the released H_2O may be incorporated into some mafic crustal rocks and preserved in the mid-lower mantle (cyan areas); at a depth of ~1,800 km, the surviving FeOOH in the very cold subducting slabs transformed into Py-FeO_2H_x (carmine region) and accumulated at the CMB (J. Liu et al., 2017). LLSVPs, large low shear velocity provinces; and ULVZs, ultralow-velocity zones.

5. Conclusions

We investigated the thermal stability of FeOOH by shock recovery experiments up to ~70 GPa and ~2,750 K in a two-stage light-gas gun. The experimental results indicate that FeOOH in the subducting slabs may decompose to release H_2O and O_2. The deoxygenation of FeOOH may be one of the sporadic sources for the GOE at ~2.3–2.5 Gyr ago. The dehydration of FeOOH may alter the physical and chemical states of the mid-lower mantle. If FeOOH forms solid solutions with some $CaCl_2$-type hydrous phases in subducting oceanic crust, it may transport water into the deep lower mantle.

Data Availability Statement

All the data to produce all the figures in this paper are available on Zenodo (http://doi.org/10.5281/zenodo.4784972). More detailed information of experimental results can be found in the Supporting Information.

Acknowledgments
The authors acknowledge Feng Gao, Xilong Dou, Yuanyuan Li, and Shangchun Shi for their help in shock experiments, Hailang Zhu for his help in thermal analysis, and Duanwei He and Li Lei for X-ray diffraction and SEM analyses. The authors thank Feng Gao and two anonymous reviewers for their constructive comments that improved this manuscript. This work was supported by the United Laboratory of High-Pressure Physics and Earthquake Science (HPPES202001) and partly funded by the Key Laboratory of Deep Earth Science and Engineering, Ministry of Education (DESEYU202104), and the National Natural Science Foundation of China (Grant No. 42074098).

References

Avice, G., Marty, B., & Burgess, R. (2017). The origin and degassing history of the Earth's atmosphere revealed by Archean xenon. *Nature Communications*, *8*(1), 15455. https://doi.org/10.1038/ncomms15455

Avice, G., Marty, B., Burgess, R., Hofmann, A., Philippot, P., Zahnle, K., & Zakharov, D. (2018). Evolution of atmospheric xenon and other noble gases inferred from Archean to Paleoproterozoic rocks. *Geochimica et Cosmochimica Acta*, *232*, 82–100. https://doi.org/10.1016/j.gca.2018.04.018

Bindeman, I. N., Zakharov, D. O., Palandri, J., Greber, N. D., Dauphas, N., Retallack, G. J., et al. (2018). Rapid emergence of subaerial landmasses and onset of a modern hydrologic cycle 2.5 billion years ago. *Nature*, *557*(7706), 545–548. https://doi.org/10.1038/s41586-018-0131-1

Brown, J. M., & McQueen, R. G. (1986). Phase transitions, Grüneisen parameter, and elasticity for shocked iron between 77 GPa and 400 GPa. *Journal of Geophysical Research*, *91*(B7), 7485–7494. https://doi.org/10.1029/JB091iB07p07485

Bykova, E., Dubrovinsky, L., Dubrovinskaia, N., Bykov, M., McCammon, C., Ovsyannikov, S. V., et al. (2016). Structural complexity of simple Fe_2O_3 at high pressures and temperatures. *Nature Communications*, *7*(1), 10661. https://doi.org/10.1038/ncomms10661

Canfield, D. E. (2004). The early history of atmospheric oxygen: Homage to Robert M. Garrels. *Annual Review of Earth and Planetary Sciences*, *33*(1), 1–36. https://doi.org/10.1146/annurev.earth.33.092203.122711

Canfield, D. E., Rosing, M. T., & Bjerrum, C. (2006). Early anaerobic metabolisms. *Philosophical Transactions of the Royal Society B: Biological Sciences*, *361*(1474), 1819–1836. https://doi.org/10.1098/rstb.2006.1906

Chang, Y.-Y., Hsieh, W.-P., Tan, E., & Chen, J. (2017). Hydration-reduced lattice thermal conductivity of olivine in Earth's upper mantle. *Proceedings of the National Academy of Sciences of the United States of America*, *114*(16), 4078–4081. https://doi.org/10.1073/pnas.1616216114

Chen, H., Xie, S.-Y., Ko, B., Kim, T., Nisr, C., Prakapenka, V., et al. (2020). A new hydrous iron oxide phase stable at mid-mantle pressures. *Earth and Planetary Science Letters*, *550*, 116551. https://doi.org/10.1016/j.epsl.2020.116551

Chen, X., Gong, Z., Fei, Y., Zhang, L., Deng, L., & Jing, F. (2006). A new evidence of the stability of (Mg, Fe)SiO_3 perovskite at lower mantle conditions: Shock recovery experiments. *AIP Conference Proceedings*, *845*(1), 1449–1452. https://doi.org/10.1063/1.2263597

Condie, K. C., Aster, R. C., & van Hunen, J. (2016). A great thermal divergence in the mantle beginning 2.5 Ga: Geochemical constraints from greenstone basalts and komatiites. *Geoscience Frontiers*, *7*, 543–553. https://doi.org/10.1016/j.gsf.2016.01.006

Croal, L. R., Johnson, C. M., Beard, B. L., & Newman, D. K. (2004). Iron isotope fractionation by Fe(II)-oxidizing photoautotrophic bacteria. *Geochimica et Cosmochimica Acta*, *68*(6), 1227–1242. https://doi.org/10.1016/j.gca.2003.09.011

Dyuzheva, T. I., Lityagina, L. M., Nikolaev, N. A., Martynov, B. N., & Bendeliani, N. A. (2006). Growth of single crystals of the high-pressure ε-FeOOH phase. *Crystallography Reports*, *51*(2), 342–343. https://doi.org/10.1134/S1063774506020234

Eguchi, J., Seales, J., & Dasgupta, R. (2020). Great Oxidation and Lomagundi events linked by deep cycling and enhanced degassing of carbon. *Nature Geoscience*, *13*(1), 71–76. https://doi.org/10.1038/s41561-019-0492-6

Ernst, R., & Bleeker, W. (2010). Large igneous provinces (LIPs), giant dyke swarms, and mantle plumes: Significance for breakup events within Canada and adjacent regions from 2.5 Ga to the Present. *Canadian Journal of Earth Sciences*, *47*(5), 695–739. https://doi.org/10.1139/E10-025

Farquhar, J., Bao, H., & Thiemens, M. (2000). Atmospheric influence of Earth's earliest sulfur cycle. *Science*, *289*(5480), 756–758. https://doi.org/10.1126/science.289.5480.756

Fu, S., Yang, J., Karato, S.-i., Vasiliev, A., Presniakov, M. Y., Gavriliuk, A. G., et al. (2019). Water concentration in single-crystal (Al, Fe)-bearing bridgmanite grown from the hydrous melt: Implications for dehydration melting at the topmost lower mantle. *Geophysical Research Letters*, *46*(17–18), 10346–10357. https://doi.org/10.1029/2019GL084630

Gleason, A. E., Jeanloz, R., & Kunz, M. (2008). Pressure-temperature stability studies of FeOOH using X-ray diffraction. *American Mineralogist*, *93*(11–12), 1882–1885. https://doi.org/10.2138/am.2008.2942

Gualtieri, A. F., & Venturelli, P. (1999). In situ study of the goethite-hematite phase transformation by real time synchrotron powder diffraction. *American Mineralogist*, *84*(5–6), 895–904. https://doi.org/10.2138/am-1999-5-624

Gumsley, A. P., Chamberlain, K. R., Bleeker, W., Söderlund, U., de Kock, M. O., Larsson, E. R., & Bekker, A. (2017). Timing and tempo of the Great Oxidation Event. *Proceedings of the National Academy of Sciences of the United States of America*, *114*(8), 1811–1816. https://doi.org/10.1073/pnas.1608824114

Guo, Q., Strauss, H., Kaufman, A., Schröder, S., Gutzmer, J., Wing, B., et al. (2009). Reconstructing Earth's surface oxidation across the Archean-Proterozoic transition. *Geology*, *37*, 399–402. https://doi.org/10.1130/G25423A.1

Heising, S., Richter, L., Ludwig, W., & Schink, B. (1999). Chlorobium ferrooxidans sp. nov., a phototrophic green sulfur bacterium that oxidizes ferrous iron in coculture with a "Geospirillum" sp. strain. *Archives of Microbiology*, *172*(2), 116–124. https://doi.org/10.1007/s002030050748

Holland, H. D. (2002). Volcanic gases, black smokers, and the great oxidation event. *Geochimica et Cosmochimica Acta*, *66*(21), 3811–3826. https://doi.org/10.1016/S0016-7037(02)00950-X

Hou, M., He, Y., Jang, B. G., Sun, S., Zhuang, Y., Deng, L., et al. (2021). Superionic iron oxide–hydroxide in Earth's deep mantle. *Nature Geoscience*, *14*(3), 174–178. https://doi.org/10.1038/s41561-021-00696-2

Hu, Q., Kim, D. Y., Liu, J., Meng, Y., Yang, L., Zhang, D., et al. (2017). Dehydrogenation of goethite in Earth's deep lower mantle. *Proceedings of the National Academy of Sciences of the United States of America*, *114*(7), 1498–1501. https://doi.org/10.1073/pnas.1620644114

Hu, Q., Kim, D. Y., Yang, W., Yang, L., Meng, Y., Zhang, L., & Mao, H.-K. (2016). FeO_2 and FeOOH under deep lower-mantle conditions and Earth's oxygen–hydrogen cycles. *Nature*, *534*(7606), 241–244. https://doi.org/10.1038/nature18018

Hwang, H., Seoung, D., Lee, Y., Liu, Z., Liermann, H.-P., Cynn, H., et al. (2017). A role for subducted super-hydrated kaolinite in Earth's deep water cycle. *Nature Geoscience*, *10*(12), 947–953. https://doi.org/10.1038/s41561-017-0008-1

Ibrahim, M. M., Edwards, G., Seehra, M. S., Ganguly, B., & Huffman, G. P. (1994). Magnetism and spin dynamics of nanoscale FeOOH particles. *Journal of Applied Physics*, *75*(10), 5873–5875. https://doi.org/10.1063/1.355545

Ikeda, O., Sakamaki, T., Ohashi, T., Goto, M., Higo, Y., & Suzuki, A. (2019). Sound velocity measurements of ε–FeOOH up to 24 GPa. *Journal of Mineralogical and Petrological Sciences*, *114*(3), 155–160. https://doi.org/10.2465/jmps.181115b

Jacobsen, S. D., & Smyth, J. R. (2006). Effect of water on the sound velocities of ringwoodite in the transition zone. In S. D. Jacobsen, & S. van der Lee (Eds.), *Earth's deep water cycle* (pp. 131–145). American Geophysical Union. https://doi.org/10.1029/168GM10

Jacobsen, S. D., Smyth, J. R., Spetzler, H., Holl, C. M., & Frost, D. J. (2004). Sound velocities and elastic constants of iron-bearing hydrous ringwoodite. *Physics of the Earth and Planetary Interiors*, *143–144*, 47–56. https://doi.org/10.1016/j.pepi.2003.07.019

Jiao, Y., Kappler, A., Croal, L., & Newman, D. (2005). Isolation and characterization of a genetically tractable photoautotrophic Fe(II)-oxidizing bacterium, rhodopseudomonas palustris strain TIE-1. *Applied and Environmental Microbiology*, *71*, 4487–4496. https://doi.org/10.1128/AEM.71.8.4487-4496.2005

Kappler, A., & Newman, D. K. (2004). Formation of Fe(III)-minerals by Fe(II)-oxidizing photoautotrophic bacteria. *Geochimica et Cosmochimica Acta*, *68*(6), 1217–1226. https://doi.org/10.1016/j.gca.2003.09.006

Karhu, J. A., & Holland, H. D. (1996). Carbon isotopes and the rise of atmospheric oxygen. *Geology*, *24*(10), 867–870. https://doi.org/10.1130/0091-7613(1996)024<0867:ciatro>2.3.co;2

Katsura, T., Yoneda, A., Yamazaki, D., Yoshino, T., & Ito, E. (2010). Adiabatic temperature profile in the mantle. *Physics of the Earth and Planetary Interiors*, *183*(1), 212–218. https://doi.org/10.1016/j.pepi.2010.07.001

Koemets, E., Fedotenko, T., Khandarkhaeva, S., Bykov, M., Bykova, E., Thielmann, M., et al. (2021). Chemical stability of FeOOH at high pressure and temperature, and oxygen recycling in early Earth history. *European Journal of Inorganic Chemistry*, *2021*(30), 3048–3048. https://doi.org/10.1002/ejic.202100274

Kohlstedt, D. L., Keppler, H., & Rubie, D. C. (1996). Solubility of water in the α, β and γ phases of $(Mg,Fe)_2SiO_4$. *Contributions to Mineralogy and Petrology*, *123*(4), 345–357. https://doi.org/10.1007/s004100050161

Komabayashi, T., Hirose, K., Funakoshi, K.-i., & Takafuji, N. (2005). Stability of phase A in antigorite (serpentine) composition determined by in situ X-ray pressure observations. *Physics of the Earth and Planetary Interiors*, *151*(3), 276–289. https://doi.org/10.1016/j.pepi.2005.04.002

Komabayashi, T., Omori, S., & Maruyama, S. (2004). Petrogenetic grid in the system MgO-SiO_2-H_2O up to 30 GPa, 1600°C: Applications to hydrous peridotite subducting into the Earth's deep interior. *Journal of Geophysical Research*, *109*(B3). https://doi.org/10.1029/2003JB002651

Konhauser, K. O., Lalonde, S. V., Planavsky, N. J., Pecoits, E., Lyons, T. W., Mojzsis, S. J., et al. (2011). Aerobic bacterial pyrite oxidation and acid rock drainage during the Great Oxidation Event. *Nature*, *478*(7369), 369–373. https://doi.org/10.1038/nature10511

Liu, J., Hu, Q., Young Kim, D., Wu, Z., Wang, W., Xiao, Y., et al. (2017). Hydrogen-bearing iron peroxide and the origin of ultralow-velocity zones. *Nature*, *551*(7681), 494–497. https://doi.org/10.1038/nature24461

Liu, J., Wang, C., Lv, C., Su, X., Liu, Y., Tang, R., et al. (2020). Evidence for oxygenation of Fe-Mg oxides at mid-mantle conditions and the rise of deep oxygen. *National Science Review*, *8*, 1–6. https://doi.org/10.1093/nsr/nwaa096

Liu, K., Dai, L., Li, H., Hu, H., Zhuang, Y., Yang, L., et al. (2019). Pressure-induced phase transitions for goethite investigated by Raman spectroscopy and electrical conductivity. *High Pressure Research*, *39*(1), 106–116. https://doi.org/10.1080/08957959.2019.1572751

Liu, X., Matsukage, K. N., Li, Y., Takahashi, E., Suzuki, T., & Xiong, X. (2018). Aqueous fluid connectivity in subducting oceanic crust at the mantle transition zone conditions. *Journal of Geophysical Research: Solid Earth*, *123*(8), 6562–6573. https://doi.org/10.1029/2018JB015973

Lu, C., & Chen, C. (2018). High-pressure evolution of crystal bonding structures and properties of FeOOH. *The Journal of Physical Chemistry Letters*, *9*(9), 2181–2185. https://doi.org/10.1021/acs.jpclett.8b00947

Lyons, T. W., Reinhard, C. T., & Planavsky, N. J. (2014). The rise of oxygen in Earth's early ocean and atmosphere. *Nature*, *506*(7488), 307–315. https://doi.org/10.1038/nature13068

Maeda, F., Ohtani, E., Kamada, S., Sakamaki, T., Hirao, N., & Ohishi, Y. (2017). Diamond formation in the deep lower mantle: A high-pressure reaction of $MgCO_3$ and SiO_2. *Scientific Reports*, *7*(1), 40602. https://doi.org/10.1038/srep40602

Majzlan, J., Lang, B. E., Stevens, R., Navrotsky, A., Woodfield, B. F., & Boerio-Goates, J. (2003). Thermodynamics of Fe oxides: Part I. Entropy at standard temperature and pressure and heat capacity of goethite (α-FeOOH), lepidocrocite (γ-FeOOH), and maghemite (γ-Fe_2O_3). *American Mineralogist*, *88*, 846–854. https://doi.org/10.2138/am-2003-5-613

Mao, H.-K., Hu, Q., Yang, L., Liu, J., Kim, D. Y., Meng, Y., et al. (2017). When water meets iron at Earth's core–mantle boundary. *National Science Review*, *4*(6), 870–878. https://doi.org/10.1093/nsr/nwx109

Marsh, S. P. (1980). *LASL shock Hugoniot data*. University of California Press.

Martinez, I., Deutsch, A., Schärer, U., Ildefonse, P., Guyot, F., & Agrinier, P. (1995). Shock recovery experiments on dolomite and thermodynamical calculations of impact induced decarbonation. *Journal of Geophysical Research*, *100*(B8), 15465–15476. https://doi.org/10.1029/95JB01151

McQueen, R. G., Marsh, S. P., Taylor, J. W., Fritz, J. N., & Carter, W. J. (1970). The equation of state of solids from shock wave studies. In R. Kinslow (Ed.), *High-velocity impact phenomena* (pp. 293–417). Academic Press. https://doi.org/10.1016/B978-0-12-408950-1.50012-4

Morris, R. V., & Lauer, H. V., Jr. (1981). Stability of goethite (α-FeOOH) and lepidocrocite (γ-FeOOH) to dehydration by UV radiation: Implications for their occurrence on the Martian surface. *Journal of Geophysical Research*, *86*(B11), 10893–10899. https://doi.org/10.1029/JB086iB11p10893

Nishi, M. (2015). Mantle hydration. *Nature Geoscience*, *8*(1), 9–10. https://doi.org/10.1038/ngeo2326

Nishi, M., Irifune, T., Tsuchiya, J., Tange, Y., Nishihara, Y., Fujino, K., & Higo, Y. (2014). Stability of hydrous silicate at high pressures and water transport to the deep lower mantle. *Nature Geoscience*, *7*(3), 224–227. https://doi.org/10.1038/ngeo2074

Nishi, M., Kuwayama, Y., Tsuchiya, J., & Tsuchiya, T. (2017). The pyrite-type high-pressure form of FeOOH. *Nature*, *547*(7662), 205–208. https://doi.org/10.1038/nature22823

Nishi, M., Tsuchiya, J., Kuwayama, Y., Arimoto, T., Tange, Y., Higo, Y., et al. (2019). Solid Solution and compression behavior of hydroxides in the lower mantle. *Journal of Geophysical Research: Solid Earth*, *124*(10), 10231–10239. https://doi.org/10.1029/2019JB018146

Nishihara, Y., & Matsukage, K. N. (2016). Iron-titanium oxyhydroxides as water carriers in the Earth's deep mantle. *American Mineralogist*, *101*(4), 919–927. https://doi.org/10.2138/am-2016-5517

Ohira, I., Ohtani, E., Sakai, T., Miyahara, M., Hirao, N., Ohishi, Y., & Nishijima, M. (2014). Stability of a hydrous δ-phase, AlOOH-$MgSiO_2(OH)_2$, and a mechanism for water transport into the base of lower mantle. *Earth and Planetary Science Letters*, *401*, 12–17. https://doi.org/10.1016/j.epsl.2014.05.059

Ohtani, E. (2020). The role of water in Earth's mantle. *National Science Review*, *7*, 224–232. https://doi.org/10.1093/nsr/nwz071

Ohtani, E., Litasov, K., Suzuki, A., & Kondo, T. (2001). Stability field of new hydrous phase, δ-AlOOH, with implications for water transport into the deep mantle. *Geophysical Research Letters*, *28*(20), 3991–3993. https://doi.org/10.1029/2001GL013397

Ono, S. (1998). Stability limits of hydrous minerals in sediment and mid-ocean ridge basalt compositions: Implications for water transport in subduction zones. *Journal of Geophysical Research*, *103*(8), 18253–18267. https://doi.org/10.1029/98jb01351

Özdemir, Ö., & Dunlop, D. J. (2000). Intermediate magnetite formation during dehydration of goethite. *Earth and Planetary Science Letters*, *177*(1), 59–67. https://doi.org/10.1016/S0012-821X(00)00032-7

Pamato, M. G., Myhill, R., Boffa Ballaran, T., Frost, D. J., Heidelbach, F., & Miyajima, N. (2015). Lower-mantle water reservoir implied by the extreme stability of a hydrous aluminosilicate. *Nature Geoscience*, *8*(1), 75–79. https://doi.org/10.1038/ngeo2306

Panero, W. R., & Caracas, R. (2017). Stability of phase H in the $MgSiO_4H_2$–AlOOH–SiO_2 system. *Earth and Planetary Science Letters*, *463*, 171–177. https://doi.org/10.1016/j.epsl.2017.01.033

Pearson, D. G., Brenker, F. E., Nestola, F., McNeill, J., Nasdala, L., Hutchison, M. T., et al. (2014). Hydrous mantle transition zone indicated by ringwoodite included within diamond. *Nature*, *507*(7491), 221–224. https://doi.org/10.1038/nature13080

Schmandt, B., Jacobsen, S. D., Becker, T. W., Liu, Z., & Dueker, K. G. (2014). Dehydration melting at the top of the lower mantle. *Science*, *344*(6189), 1265–1268. https://doi.org/10.1126/science.1253358

Seiler, F., & Igra, O. (2016). *Hypervelocity launchers*. Springer International Publishing.

Sekine, T., Kimura, T., Kobayashi, T., & Mashimo, T. (2015). Dynamic water loss of antigorite by impact process. *Icarus*, *250*, 1–6. https://doi.org/10.1016/j.icarus.2014.11.008

Smyth, J. R. (1987). Beta-Mg_2SiO_4; a potential host for water in the mantle? *American Mineralogist*, *72*(11–12), 1051–1055

Straub, K., Rainey, F., & Widdel, F. (1999). Rhodovulum iodosum sp. nov. and Rhodovulum robiginosum sp. nov., two new marine phototrophic ferrous-iron-oxidizing purple bacteria. *International Journal of Systematic Bacteriology*, *49*, 729–735. https://doi.org/10.1099/00207713-49-2-729

Suzuki, A. (2010). High-pressure X-ray diffraction study of ε-FeOOH. *Physics and Chemistry of Minerals*, *37*(3), 153–157. https://doi.org/10.1007/s00269-009-0319-x

Thompson, A. B. (1992). Water in the Earth's upper mantle. *Nature*, *358*, 295–302. https://doi.org/10.1038/358295a0

Thompson, E. C., Davis, A. H., Brauser, N. M., Liu, Z., Prakapenka, V. B., & Campbell, A. J. (2020). Phase transitions in ε-FeOOH at high pressure and ambient temperature. *American Mineralogist*, *105*(12), 1769–1777. https://doi.org/10.2138/am-2020-7468

van der Meer, D. G., Spakman, W., van Hinsbergen, D. J. J., Amaru, M. L., & Torsvik, T. H. (2010). Towards absolute plate motions constrained by lower-mantle slab remnants. *Nature Geoscience*, *3*(1), 36–40. https://doi.org/10.1038/ngeo708

Voigt, R., & Will, G. (1981). The system Fe_2O_3-H_2O under high pressures. *Neues Jahrbuch für Mineralogie*, *2*, 89–96.

Walter, D., Buxbaum, G., & Laqua, W. (2001). The mechanism of the thermal transformation from goethite to hematite. *Journal of Thermal Analysis and Calorimetry*, *63*(3), 733–748. https://doi.org/10.1023/A:1010187921227

Watanabe, Y., & Ishii, K. (1995). Geometrical consideration of the crystallography of the transformation from α-Fe_2O_3 to Fe_3O_4. *Physica Status Solidi*, *150*(2), 673–686. https://doi.org/10.1002/pssa.2211500210

Weber, K. A., Achenbach, L. A., & Coates, J. D. (2006). Microorganisms pumping iron: Anaerobic microbial iron oxidation and reduction. *Nature Reviews Microbiology*, *4*(10), 752–764. https://doi.org/10.1038/nrmicro1490

Widdel, F., Schnell, S., Heising, S., Ehrenreich, A., Assmus, B., & Schink, B. (1993). Ferrous iron oxidation by anoxygenic phototrophic bacteria. *Nature*, *362*(6423), 834–836. https://doi.org/10.1038/362834a0

Wiethoff, F., Grevel, K.-D., Marler, B., Herrmann, J., Majzlan, J., Kirste, J., & Lathe, C. (2017). P-V-T behavior of FeO(OH) and MnO(OH). *Physics and Chemistry of Minerals*, *44*(8), 567–576. https://doi.org/10.1007/s00269-017-0884-3

Wolska, E. (1988). Relations between the existence of hydroxyl ions in the anionic sublattice of hematite and its infrared and X-ray characteristics. *Solid State Ionics*, *28–30*, 1349–1351. https://doi.org/10.1016/0167-2738(88)90385-2

Wolska, E., & Schwertmann, U. (1989). Nonstoichiometric structures during dehydroxylation of goethite. *Zeitschrift für Kristallographie—Crystalline Materials*, *189*(3–4), 223–237. https://doi.org/10.1524/zkri.1989.189.3-4.223

Xu, C., Nishi, M., & Inoue, T. (2019). Solubility behavior of δ-AlOOH and ε-FeOOH at high pressures. *American Mineralogist*, *104*(10), 1416–1420. https://doi.org/10.2138/am-2019-7064

Yoshino, T., Baker, E., & Duffey, K. (2019). Fate of water in subducted hydrous sediments deduced from stability fields of FeOOH and AlOOH up to 20 GPa. *Physics of the Earth and Planetary Interiors*, *294*, 106295. https://doi.org/10.1016/j.pepi.2019.106295

Yuan, H., Zhang, L., Ohtani, E., Meng, Y., Greenberg, E., & Prakapenka, V. B. (2019). Stability of Fe-bearing hydrous phases and element partitioning in the system MgO–Al_2O_3–Fe_2O_3–SiO_2–H_2O in Earth's lowermost mantle. *Earth and Planetary Science Letters*, *524*, 115714. https://doi.org/10.1016/j.epsl.2019.115714

Zhang, F., & Sekine, T. (2007). Impact-shock behavior of Mg- and Ca-sulfates and their hydrates. *Geochimica et Cosmochimica Acta*, *71*(16), 4125–4133. https://doi.org/10.1016/j.gca.2007.06.037

Zhang, W.-J., Huo, C.-F., Feng, G., Li, Y.-W., Wang, J., & Jiao, H. (2010). Dehydration of goethite to hematite from molecular dynamics simulation. *Journal of Molecular Structure: THEOCHEM*, *950*(1), 20–26. https://doi.org/10.1016/j.theochem.2010.03.013

Zhang, Y., Sekine, T., & He, H. (2014). A new interpretation of decomposition products of serpentine under shock compression. *American Mineralogist*, *99*(11–12), 2374–2377. https://doi.org/10.2138/am-2014-5021